

8. Reize P, Leichtle CI, Leichtle UG, Schanbacher J. Long-term results after metatarsal head resection in the treatment of rheumatoid arthritis. *Foot Ankle Int.* 2006;27(8):586–90.
9. Bibbo C, Jaffe L, Goldkind A. Complications of digital and lesser metatarsal surgery. *Clin Podiatr Med Surg.* 2010;27(4):485–507.
10. Reeves CL, Peadar AJ, Shane AM. The complications encountered with the rheumatoid surgical foot and ankle. *Clin Podiatr Med Surg.* 2010;27(2):313–25.
11. Arnett FC, Edworthy SM, Bloch DA, McShane DJ, Fries JF, Cooper NS, et al. The American Rheumatism Association 1987 revised criteria for the classification of rheumatoid arthritis. *Arthritis Rheum.* 1988;31(3):315–24.
12. Aletaha D, Neogi T, Silman AJ, Funovits J, Felson DT, Bingham CO III, et al. 2010 Rheumatoid arthritis classification criteria: an American College of Rheumatology/European League Against Rheumatism collaborative initiative. *Arthritis Rheum.* 2010;62(9):2569–81.
13. Thomas S, Kinninmonth AW, Kumar CS. Long-term results of the modified Hoffman procedure in the rheumatoid forefoot. *J Bone Joint Surg Am.* 2005;87(4):748–52.
14. Nagashima M, Kato K, Miyamoto Y, Takenouchi K. A modified Hohmann method for hallux valgus and telescoping osteotomy for lesser toe deformities in patients with rheumatoid arthritis. *Clin Rheumatol.* 2007;26(5):748–52.
15. Larsen A, Dale K, Eek M. Radiographic evaluation of rheumatoid arthritis and related conditions by standard reference films. *Acta Radiol Diagn.* 1977;18(4):481–91.
16. Nassar J, Cracchiolo A III. Complications in surgery of the foot and ankle in patients with rheumatoid arthritis. *Clin Orthop Relat Res.* 2001;(391):140–52.
17. Guo S, DiPietro LA. Factors affecting wound healing. *J Dent Res.* 2010;89(3):219–29.
18. Bibbo C, Goldberg JW. Infectious and healing complications after elective orthopaedic foot and ankle surgery during tumor necrosis factor-alpha inhibition therapy. *Foot Ankle Int.* 2004;25(5):331–5.

## Discordance and accordance between patient's and physician's assessments in rheumatoid arthritis

M Furu<sup>1,2</sup>, M Hashimoto<sup>1</sup>, H Ito<sup>1,2</sup>, T Fujii<sup>1,3</sup>, C Terao<sup>4</sup>, N Yamakawa<sup>3</sup>, H Yoshitomi<sup>2,5</sup>, H Ogino<sup>2</sup>, M Ishikawa<sup>2</sup>, S Matsuda<sup>2</sup>, T Mimori<sup>1,3</sup>

<sup>1</sup>Department of the Control for Rheumatic Diseases, <sup>2</sup>Department of Orthopaedic Surgery, <sup>3</sup>Department of Rheumatology and Clinical Immunology, <sup>4</sup>Centre for Genomic Medicine, and <sup>5</sup>Centre for Innovation in Immunoregulatory Technology and Therapeutics, Kyoto University Graduate School of Medicine, Kyoto, Japan

**Objectives:** The American College of Rheumatology/European League Against Rheumatism (ACR/EULAR) remission criteria for rheumatoid arthritis (RA) are more stringent than index-based criteria, making it more difficult to achieve a patient's global assessment (PGA) than an evaluator's global assessment (EGA). We investigated the reason for the discrepancy between the PGA and the EGA in a Japanese clinical cohort.

**Method:** We assessed clinical and laboratory variables in our clinical cohort. The frequency of remission achievement according to the ACR/EULAR remission criteria and predictors of the discrepancy between the PGA and EGA were analysed.

**Results:** Of 370 patients with RA, 89 fulfilled PGA criteria and 167 patients fulfilled EGA criteria. The PGA was highly correlated with the visual analogue scale (VAS) pain score and non-inflammatory variables including Steinbrocker class and the Health Assessment Questionnaire Disability Index (HAQ-DI). Conversely, inflammatory variables, including swollen joint count (SJC), tender joint count (TJC), and C-reactive protein (CRP) levels, were significantly associated with the EGA. The main predictors of the discrepancy between the PGA and the EGA were patient's VAS pain score, SJC, and functional disability.

**Conclusions:** Increased pain and functional disability led to a discrepancy towards a worse PGA than EGA, whereas increased SJC led to an accordance towards a worse EGA.

Rheumatoid arthritis (RA) is an inflammatory systematic disease that is characterized by swelling and tenderness of the synovial joints, leading to joint destruction, disability, and reduced quality of life (1). Recently, new remission criteria were presented by the American College of Rheumatology (ACR) and the European League Against Rheumatism (EULAR) (2). Some studies have reported that the new ACR/EULAR remission criteria are problematic with regard to achieving the patient's global assessment (PGA) (3). In daily clinical practice, it is frequently observed that the PGA is higher than expected based on patients' clinical disease activity. Patients and physicians often differ in their perceptions of disease activity as quantified by the PGA and the evaluator's global assessment (EGA), respectively (4). Understanding the reasons for these discrepancies between the PGA and EGA becomes particularly important in the context of recent recommendations that define remission as the treatment

target (5). Taking all of these concerns into consideration, the aim of the present study was to determine the factors that underlie the observed discrepancy between the PGA and the EGA in our observational cohort.

### Method

#### Patients and data

We enrolled our patients from the Kyoto University Rheumatoid Arthritis Management Alliance (KURAMA) cohort (6). Clinical and laboratory variables that are characteristic of RA are assessed and documented every year for an RA survey, which includes a patient-based questionnaire. In 2012, a total of 384 patients with RA were enrolled in the RA survey. All of the patients fulfilled the revised 1987 ACR criteria for RA (7) or the 2010 ACR/EULAR classification criteria for RA (8). These patients were being treated by rheumatologists.

Information on demographic features and clinical and laboratory variables was extracted from the KURAMA cohort. These data included age, sex, disease duration, Steinbrocker class, Steinbrocker stage, the 28-swollen joint count (SJC28), 28-tender joint count (TJC28),

Moritoshi Furu, Department of the Control for Rheumatic Diseases, Kyoto University Graduate School of Medicine, 54 Kawahara-cho, Shogoin, Sakyo, Kyoto 606-8507, Japan.  
E-mail: morifuru@kuhp.kyoto-u.ac.jp

Accepted 24 November 2013

presence of rheumatoid factor (RF) and/or anti-cyclic citrullinated protein (anti-CCP) antibodies, C-reactive protein (CRP) level, erythrocyte sedimentation rate (ESR), score on the Health Assessment Questionnaire Disability Index (HAQ-DI), patient's assessment of pain [measured using a 100-mm visual analogue scale (VAS)], and global assessments of disease activity by evaluators (EGA) and patients (PGA). To analyse discrepancies between the PGA and the EGA, we calculated the 'PGA minus EGA' (PGA – EGA) variable (5). Van der Heijde/modified Sharp scores were available for radiographic data. Clinical remission was defined as a 28-joint Disease Activity Score (DAS28) < 2.6, Simple Disease Activity Index (SDAI)  $\leq$  3.3, Clinical Disease Activity Index (CDAI)  $\leq$  2.8, or Boolean-based remission criteria (28 tender and swollen joint counts, PGA and CRP all  $\leq$  1). Only patients with a complete dataset were used in our analyses.

This study was designed in accordance with the Declaration of Helsinki and its consent procedure was approved by the ethics committee of the Kyoto University Graduate School and Faculty of Medicine.

### Statistical analyses

To identify variables that were correlated with the PGA, EGA and PGA – EGA, we calculated Pearson's correlation coefficients for continuous variables or Spearman's rank correlation coefficient for ordinal variables. Subsequently, the significant variables identified in this univariate correlation were tested in multivariate analyses for between-subject effects, and were tested further by linear multivariate regression modelling. In these models, variables were selected using a cut-off point of  $p < 0.001$  for entry into the multivariate regression models. All analyses were performed using JMP software, version 10.0.2.

## Results

### Study population

In total, we enrolled 384 patients in the RA survey in 2012, and complete datasets for 370 of these patients were used in this study. The demographic characteristics of the patients are shown in Table 1. The proportions of patients who fulfilled the remission criteria are shown in Table 2.

### Functional remission was most achievable in patients who fulfilled Boolean-based remission

Values of the HAQ-DI for patients who fulfilled Boolean-based remission were the lowest among the remission criteria. Functional remission (HAQ-DI  $\leq$  0.5) was achieved in 87 (67.9%), 75 (80.6%), 76 (81.7%), and 52

(81.3%) patients who fulfilled the remission criteria according to DAS28, CDAI, SDAI, and Boolean-based remission, respectively. Patients who fulfilled three of the four Boolean criteria (after elimination of the PGA) had a lower functional remission rate (60.0%) than those who fulfilled the four Boolean criteria (Table 2).

### Determinants of PGA or EGA

Univariate analyses showed that non-inflammatory variables (including Steinbrocker class and HAQ-DI), inflammatory variables (including TJC28 and SJC28), and VAS pain score were significantly associated ( $p < 0.001$  for each variable) with PGA score (Table 3). EGA was significantly associated with non-inflammatory variables (including Steinbrocker stage, Steinbrocker class, and HAQ-DI), inflammatory variables (including TJC, SJC, CRP and ESR), and pain score. Among all of the variables, pain score exhibited the strongest correlation with PGA score. By contrast, SJC, one of the inflammatory variables, exhibited the strongest correlation with EGA score.

A subsequent multivariate regression model revealed that all variables that were significant at  $p < 0.001$  in the univariate correlation were predictors. In this model, pain score ( $t = 15.05$ ,  $p < 0.0001$ ) and Steinbrocker class ( $t = 2.71$ ,  $p = 0.0071$ ) remained significant determinants of the PGA. Regarding the EGA, the contributions of the above-mentioned variables were very different from their contributions to the PGA: the determinants of the EGA were pain score ( $t = 3.09$ ,  $p = 0.0022$ ), TJC ( $t = 8.89$ ,  $p < 0.0001$ ), SJC ( $t = 12.60$ ,  $p < 0.0001$ ), CRP level ( $t = 2.21$ ,  $p = 0.0277$ ), and ESR ( $t = 2.88$ ,  $p = 0.0042$ ).

### Determinants of the discrepancies between PGA and EGA

Our cohort exhibited discrepancies between the PGA and the EGA. Two hundred and eighty-five patients had higher PGA scores whereas 85 patients had higher EGA scores or concordant scores (Table 1). Univariate analyses showed that Steinbrocker class, HAQ-DI, SJC, and pain score were significantly associated ( $p < 0.001$  for each variable) with the PGA – EGA value (Table 3). The SJC was the only variable that showed a significant negative correlation with this value, indicating that a higher number of SJC led to a worse perception of disease activity by evaluators than patients. The other variables, which exhibited a positive correlation with this value, led to a worse perception by patients than evaluators.

Multivariate analyses indicated that the pain score ( $t = 12.03$ ,  $p < 0.0001$ ), Steinbrocker class ( $t = 2.55$ ,  $p = 0.0113$ ), and SJC ( $t = -8.90$ ,  $p < 0.0001$ ) were significantly and independently associated with the PGA – EGA value.

Table 1. Characteristics of the patient population (n = 370).

	Mean ± SD or n (%)	Median (range)
Age (years)	62.9 ± 13.0	64.5 (23–92)
Disease duration (years)	14.4 ± 11.6	13 (0–64)
≤ 2 years	48 (13.0)	
> 2 to ≤ 10 years	100 (27.0)	
> 10 years	222 (60.0)	
Women	324 (87.6)	
Steinbrocker stage, I/II/III/IV	60 (16.2)/88 (23.8)/63 (17.0)/159 (43.0)	
Steinbrocker class, 1/2/3/4	90 (24.3)/211 (57.0)/66 (17.8)/3 (0.01)	
RF positive	300 (81.1)	
Anti-CCP antibody positive	303 (81.9)	
CRP (mg/dL)	0.63 ± 1.23	0.2 (0–11.7)
Fulfilled CRP ≤ 1 mg/dL	309 (83.5)	
ESR (mm/h)	26.9 ± 22.3	20 (1–115)
TJC (0 to 28 joints)	1.2 ± 1.9	1 (0–12)
Fulfilled TJC28 ≤ 1	265 (71.6)	
SJC (0 to 28 joints)	1.4 ± 2.1	1 (0–12)
Fulfilled SJC28 ≤ 1	252 (68.1)	
PGA (0 to 100 mm)	34.9 ± 25.9	30.5 (0–100)
Fulfilled PGA ≤ 1 cm	89 (24.1)	
EGA (0 to 100 mm)	16.7 ± 15.6	12 (0–90)
Fulfilled EGA ≤ 1 cm	167 (45.1)	
PGA minus EGA (–100 to +100 mm)	18.2 ± 24.1	15 (–44 to 87)
Patient's pain VAS (0 to 100 mm)	32.2 ± 27.0	25 (0–100)
DAS28	3.21 ± 1.16	3.16 (0.08–6.59)
SDAI	8.41 ± 6.72	7.30 (0–40.5)
CDAI	7.78 ± 6.20	6.90 (0–35.4)
HAQ-DI (0 to 3)	0.84 ± 0.78	0.625 (0–3)
Sharp/van der Heijde score (n = 365)	112.1 ± 108.0	72 (0–443)
Use of glucocorticoid	150 (40.5)	
Use of methotrexate	262 (70.8)	
Use of biologics	109 (29.5)	
TNF inhibitors	66 (17.8)	
Tocilizumab	23 (6.2)	
Abatacept	20 (5.4)	

RF, Rheumatoid factor; CCP, cyclic citrullinated protein; CRP, C-reactive protein; ESR, erythrocyte sedimentation rate; TJC, tender joint count; SJC, swollen joint count; PGA, patient's global assessment; EGA, evaluator's global assessment; VAS, visual analogue scale; DAS28, Disease Activity Score in 28 joints; SDAI, Simplified Disease Activity Index; CDAI, Clinical Disease Activity Index; HAQ-DI, Health Assessment Questionnaire Disability Index; TNF, tumour necrosis factor.

Table 2. Proportions and characteristics of patients who fulfilled each criterion.

		DAS28 remission	CDAI remission	SDAI remission	Boolean remission	CRP ≤ 1, TJC ≤ 1, and SJC ≤ 1
Fulfilled	n (%)	128 (34.6)	93 (25.1)	93 (25.1)	64 (17.3)	190 (50.8)
PGA (0 to 100 mm)	median (range)	11.5 (0–78)	7 (0–26)	7 (0–26)	4.5 (0–10)	18 (0–100)
Fulfilled PGA ≤ 1 cm	n (%)	61 (47.6)	61 (65.5)	61 (65.5)	64 (100)	64 (33.7)
EGA (0 to 100 mm)	median (range)	5 (0–46)	4 (0–17)	4 (0–17)	4 (0–46)	6 (0–46)
Fulfilled EGA ≤ 1 cm	n (%)	104 (81.2)	90 (96.7)	89 (95.7)	56 (87.5)	145 (76.3)
PGA minus EGA (–100 to +100 mm)	median (range)	5 (–40 to 69)	3 (–13 to 25)	3 (–13 to 25)	0 (–40 to 9)	10.5 (–40 to 87)
Pain VAS (0 to 100 mm)	median (range)	8 (0–100)	6 (0–88)	6 (0–88)	4 (0–61)	13 (0–100)
TJC28 (0 to 28 joints)	median (range)	0 (0–2)	0 (0–1)	0 (0–2)	0 (0–1)	0 (0–1)
Fulfilled TJC ≤ 1	n (%)	122 (95.3)	93 (100)	92 (98.9)	64 (100)	190 (100)
SJC28 (0 to 28 joints)	median (range)	0 (0–3)	0 (0–1)	0 (0–1)	0 (0–1)	0 (0–1)
Fulfilled SJC ≤ 1	n (%)	124 (96.8)	93 (100)	93 (100)	64 (100)	190 (100)
CRP (mg/dL)	mean (SD)	0.12 (0.24)	0.30 (0.74)	0.15 (0.26)	0.13 (0.20)	0.16 (0.21)
Fulfilled CRP ≤ 1 mg/dL	n (%)	126 (98.4)	88 (94.6)	92 (98.9)	64 (100)	190 (100)
ESR (mm/h)	mean (SD)	11.4 (7.2)	19.3 (19.0)	17.0 (16.3)	17.9 (18.0)	17.9 (15.5)
HAQ-DI (0 to 3)	mean (SD)	0.47 (0.61)	0.32 (0.51)	0.32 (0.50)	0.29 (0.48)	0.58 (0.67)
Functional remission	n (%)	87 (67.9)	75 (80.6)	76 (81.7)	52 (81.3)	114 (60.0)

DAS28, Disease Activity Score in 28 joints (DAS28 remission: DAS28 < 2.6); SDAI, Simplified Disease Activity Index (SDAI remission: SDAI ≤ 3.3); CDAI, Clinical Disease Activity Index (CDAI remission, CDAI ≤ 2.8); PGA, patient's global assessment; EGA, evaluator's global assessment; VAS, visual analogue scale; TJC28, tender joint count in 28 joints; SJC28, swollen joint count in 28 joints; CRP, C-reactive protein; ESR, erythrocyte sedimentation rate; HAQ-DI, Health Assessment Questionnaire Disability Index (functional remission was configured using HAQ-DI ≤ 0.5); SD, standard deviation.

Table 3. Correlation of clinical variables with the patient's and evaluator's global assessment.

	Correlation coefficient		
	PGA	EGA	PGA minus EGA
Age	0.163*	0.053	0.140
Disease duration	0.158*	0.191†	0.045
Steinbrocker stage	0.168*	0.298†	0.029
Steinbrocker class	0.533†	0.389†	0.365†
HAQ-DI	0.462†	0.385†	0.247†
Pain VAS	0.746†	0.407†	0.537†
TJC28	0.350†	0.635†	-0.036
SJC28	0.250†	0.719†	-0.197†
CRP	0.125	0.408†	-0.130
ESR	0.192†	0.381†	-0.040

Data represent Pearson's correlation coefficient (*r*) or Spearman's rank correlation coefficient (*ρ*) for the patient's global assessment (PGA), the evaluator's global assessment (EGA), and PGA minus EGA in the 370 patients included in our clinical cohort.

HAQ-DI, Health Assessment Questionnaire Disability Index; VAS, visual analogue scale; TJC28, tender joint count in 28 joints; SJC28, swollen joint count in 28 joints; CRP, C-reactive protein; ESR, erythrocyte sedimentation rate.

\**p* < 0.005, †*p* < 0.001.

## Discussion

The ACR/EULAR remission criteria were designed to be rigorous criteria aimed at resolving the controversies that were inherent to previous definitions (2). Some studies have demonstrated that a considerable proportion of patients do not achieve Boolean-based remission because the PGA criteria were not fulfilled (3, 9). Boolean-based remission was achieved in one-sixth of patients, while half of the patients fulfilled three of the four Boolean criteria after the elimination of the PGA in our cohort (v2). Meanwhile, the DAS28 and the ACR/EULAR remission criteria contain only 28 joints and omit joints of the ankle and foot. Residual foot synovitis was present in a substantial proportion of RA patients who fulfilled the 28-joint count criteria for remission (10). The PGA may be higher in RA patients with residual foot synovitis.

In our multivariate analysis, the patient's pain score and the Steinbrocker class were the most important determinants of the PGA, whereas the SJC and the TJC were the most important determinants for the EGA. Although the patient's pain may also include tenderness of the joints, the TJC affected only the EGA but not the PGA in this study. This suggests that the patient's pain may originate not only from synovitis, which causes joint tenderness, but also from joint damage, which causes joint pain during motion. The omission of pain from the multivariate analysis led to the appearance of HAQ-DI and the Steinbrocker class as the most important predictors for the PGA. Long-standing RA is usually associated with more severe joint destruction, which decreases the quality of life and increases the damage-related

component of the HAQ, improvement of which is difficult (11). The PGA score was higher in patients with a high HAQ-DI and long disease duration in this study.

Patients and physicians differ in their perceptions of disease activity, as quantified by the PGA and the EGA, respectively (4, 12). Our multivariate analysis demonstrated that discordance between the PGA and the EGA was increased with elevated pain scores but decreased with elevated SJC. This may be because the EGA mainly depends upon the SJC, which reflects the disease activity, whereas the PGA is influenced by pain, which reflects not only disease activity but also non-reversible functional disability. The PGA is important for understanding the patient's priorities and problems, including pain and functional disability. Physicians should attend to patient's demands and make an informed decision regarding RA treatment.

In conclusion, the PGA is important to achieving RA remission according to the new ACR/EULAR criteria. Patients and physicians differ in their perceptions of disease activity. Understanding the reasons for the discordance observed between patients and physicians may help to facilitate the management of RA.

## Acknowledgements

We thank K Yamamoto at the Division of Clinical and Epidemiology, Department of Health Information Governance, National Cerebral and Cardiovascular Centre, and W Yamamoto at the Kurashiki Sweet Hospital, for their support in the establishment and maintenance of the KURAMA cohort. We also thank K Ohmura and K Murakami at the Department of Rheumatology and Clinical Immunology, Kyoto University Graduate School of Medicine, for advice regarding radiographic analysis. Finally, we thank M Hamaguchi at the Department of Experimental Immunology, Immunology Frontier Research Centre, Osaka University, for his instructions and advice regarding the statistical analyses.

## References

1. Scott DL, Pugno K, Kaarela K, Doyle DV, Woolf A, Holmes J, et al. The links between joint damage and disability in rheumatoid arthritis. *Rheumatology (Oxford)* 2000;39:122–32.
2. Felson DT, Smolen JS, Wells G, Zhang B, van Tuyl LH, Funovits J, et al. American College of Rheumatology/European League Against Rheumatism provisional definition of remission in rheumatoid arthritis for clinical trials. *Ann Rheum Dis* 2011;70:404–13.
3. Masri KR, Shaver TS, Shahouri SH, Wang S, Anderson JD, Busch RE, et al. Validity and reliability problems with patient global as a component of the ACR/EULAR remission criteria as used in clinical practice. *J Rheumatol* 2012;39:1139–45.
4. Studenic P, Radner H, Smolen JS, Aletaha D. Discrepancies between patients and physicians in their perceptions of rheumatoid arthritis disease activity. *Arthritis Rheum* 2012;64:2814–23.
5. Smolen JS, Aletaha D, Bijlsma JW, Breedveld FC, Boumpas D, Burmester G, et al. Treating rheumatoid arthritis to target: recommendations of an international task force. *Ann Rheum Dis* 2010;69:631–7.
6. Terao C, Hashimoto M, Yamamoto K, Murakami K, Ohmura K, Nakashima R, et al. Three groups in the 28 joints for rheumatoid arthritis synovitis – analysis using more than 17,000 assessments in the KURAMA database. *PLoS One* 2013;8:e59341.

7. Arnett FC, Edworthy SM, Bloch DA, McShane DJ, Fries JF, Cooper NS, et al. The American Rheumatism Association 1987 revised criteria for the classification of rheumatoid arthritis. *Arthritis Rheum* 1988;31:315–24.
8. Aletaha D, Neogi T, Silman AJ, Funovits J, Felson DT, Bingham CO 3rd, et al. 2010 Rheumatoid arthritis classification criteria: an American College of Rheumatology/European League Against Rheumatism collaborative initiative. *Arthritis Rheum* 2010;62:2569–81.
9. Studenic P, Smolen JS, Aletaha D. Near misses of ACR/EULAR criteria for remission: effects of patient global assessment in Boolean and index-based definitions. *Ann Rheum Dis* 2012;71:1702–5.
10. Wechalekar MD, Lester S, Proudman SM, Cleland LG, Whittle SL, Rischmueller M, et al. Active synovitis in patients with rheumatoid arthritis. *Arthritis Rheum* 2012;64:1316–22.
11. Smolen JS, Aletaha D, Grisar JC, Stamm TA, Sharp JT. Estimation of a numerical value for joint damage-related physical disability in rheumatoid arthritis clinical trials. *Ann Rheum Dis* 2010;69:1058–64.
12. Rohekar G, Pope J. Test-related reliability of patient global assessment and physician global assessment in rheumatoid arthritis. *J Rheumatol* 2009;36:2178–82.



ELSEVIER

# The anatomy of the coracohumeral ligament and its relation to the subscapularis muscle



Ryuzo Arai, MD<sup>a</sup>, Akimoto Nimura, MD, PhD<sup>b</sup>, Kumiko Yamaguchi, MD, PhD<sup>b</sup>, Hideya Yoshimura, MD, PhD<sup>c</sup>, Hiroyuki Sugaya, MD, PhD<sup>d</sup>, Takahiko Saji, MD<sup>a</sup>, Shuichi Matsuda, MD, PhD<sup>a</sup>, Keiichi Akita, MD, PhD<sup>b,\*</sup>

<sup>a</sup>Department of Orthopaedic Surgery, Kyoto University, Kyoto, Japan

<sup>b</sup>Department of Clinical Anatomy, Graduate School of Medical and Dental Sciences, Tokyo Medical and Dental University, Tokyo, Japan

<sup>c</sup>Department of Orthopaedic Surgery, Kawaguchi Kogyo General Hospital, Kawaguchi, Japan

<sup>d</sup>Shoulder and Elbow Service, Funabashi Orthopaedic Sports Medicine Center, Funabashi, Japan

**Background:** Only a few reports describe the extension of the coracohumeral ligament to the subscapularis muscle. The purposes of this study were to histo-anatomically examine the structure between the ligament and subscapularis and to discuss the function of the ligament.

**Methods:** Nineteen intact embalmed shoulders were used. In 9 shoulders, the expansion of the ligament was anatomically observed, and in 6 of these 9, the muscular tissue of the supraspinatus and subscapularis was removed to carefully examine the attachments to the tendons of these muscles. Five shoulders were frozen and sagittally sectioned into 3-mm-thick slices. After observation, histologic analysis was performed on 3 of these shoulders. In the remaining 5 shoulders, the coracoid process was harvested to investigate the ligament origin.

**Results:** The coracohumeral ligament originated from the horizontal limb and base of the coracoid process and enveloped the cranial part of the subscapularis muscle. The superficial layer of the ligament covered a broad area of the anterior surface of the muscle. Laterally, it protruded between the long head of the biceps tendon and subscapularis and attached to the tendinous floor, which extended from the subscapularis insertion. Histologically, the ligament consisted of irregular and sparse fibers abundant in type III collagen.

**Conclusion:** The coracohumeral ligament envelops the whole subscapularis muscle and insertion and seems to function as a kind of holder for the subscapularis and supraspinatus muscles. The ligament is composed of irregular and sparse fibers and contains relatively rich type III collagen, which would suggest flexibility.

**Level of evidence:** Basic Science, Anatomy.

© 2014 Journal of Shoulder and Elbow Surgery Board of Trustees.

**Keywords:** Anatomy; histology; shoulder joint; subscapularis muscle; coracohumeral ligament; collagen

This study used cadaveric specimens with full consent for study. There was no need for approval from the institutional review board or ethical committee in terms of ethical considerations.

\*Reprint requests: Keiichi Akita, MD, PhD, Department of Clinical Anatomy, Graduate School of Medical and Dental Sciences, Tokyo

Medical and Dental University, 1-5-45, Yushima, Bunkyo-ku, Tokyo 113-8519, Japan.

E-mail address: akita.fana@tmd.ac.jp (K. Akita).

The coracohumeral ligament (CHL) was classically described to originate in the outer margin of the horizontal limb of the coracoid process, insert into the greater and lesser tubercles,<sup>9</sup> and cover the rotator interval, which is the space between the supraspinatus and subscapularis muscles. The CHL was considered to play a key role in the function of the rotator interval.<sup>15</sup> In a biomechanical study, Harryman et al<sup>13</sup> showed that the tension of the CHL has a great effect on the stability and range of motion of the glenohumeral joint. In fact, it was clinically reported that dysfunction of the CHL can lead to “frozen” shoulder or a kind of loose shoulder.<sup>7,19</sup>

The posterior extension of the CHL from the rotator interval has become well known since the anatomic study of Clark and Harryman.<sup>5</sup> Their study showed that both the superficial and deep branches of the CHL envelop the anterior part of the supraspinatus tendon; the superficial branch fans out laterally and posteriorly over the supraspinatus tendon, extending as far as the infraspinatus, and merges with the periosteum of the greater tubercle. This envelop-like structure of the CHL should act as a stabilizer of the posterosuperior side of the glenohumeral joint.

However, to date, studies focusing on the anteriorly extending fibers of the CHL are few. Recently, Yang et al<sup>24</sup> macroscopically examined the insertion of the ligament-like portion of the CHL in 26 fresh-frozen cadavers. They showed that in 3 shoulders, the ligament-like CHL bifurcated and inserted into both the supraspinatus and subscapularis tendons. Interestingly, in 1 specimen, the ligament inserted only into the subscapularis tendon. They, however, did not show the continuity between the ligament-like CHL insertion into the subscapularis and the membranous portion of the CHL in the rotator interval. Furthermore, the expansion of the CHL around the subscapularis muscle was not shown. Arai et al<sup>1</sup> reported on the soft tissue composing the CHL, which bridged over the cranial part of the subscapularis muscle, but to date, there is no clear report on the detailed structure of the anterior CHL. Considering the dynamic function of the subscapularis muscle to maintain the balanced “force couple” between the anterior and posterior rotator cuff muscles<sup>3,14</sup> and the consistency of the function in any position of the upper limb, it would be expected that the anteriorly extending component of the CHL has an appropriate structure sufficient to hold the subscapularis, just as the posterior portion of the ligament has the configuration to hold the supraspinatus muscle.

The purposes of this study were to closely observe the anteriorly extending fibers of the CHL anatomically and histologically and to examine the role of the CHL in the stabilization of the subscapularis muscle.

## Materials and methods

All of the cadavers used in this study were donated to the Department of Anatomy, Tokyo Medical and Dental University.

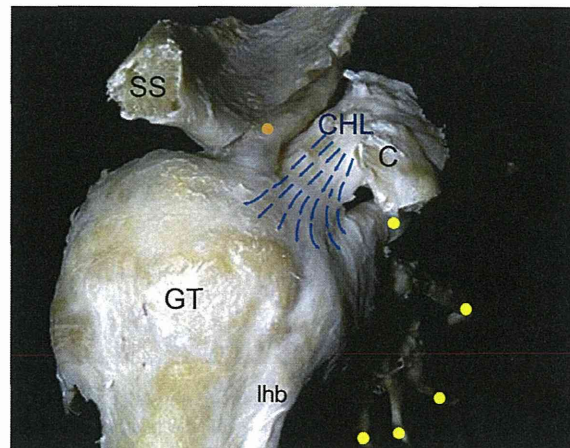


**Figure 1** Anatomy of CHL. A right shoulder viewed from the lateral side is shown. The scapular spine (SS) was cut, and the muscular tissue of the supraspinatus and subscapularis was carefully removed. The CHL originated from the coracoid process (C). The CHL extended over not only the rotator interval but also the cranial part of the subscapularis muscle (*blue arrows*). It covered a broad area of the anterior surface of the subscapularis muscle. The *orange circle* indicates the intramuscular tendon of the supraspinatus, and the *yellow circles* indicate the intramuscular tendons of the subscapularis. GT, Greater tuberosity; lhb, long head of biceps brachii tendon.

All of the donors voluntarily expressed their will, before death, that their remains be used as materials for education and study. This voluntary donor system of cadavers is widespread throughout Japan, and our study completely complied with the current laws of Japan. A history of any shoulder problem was not available.

All cadavers were fixed in 8% formalin and preserved in 30% ethanol. First, 8 cadavers (4 males and 4 females; mean age, 78.0 years) were randomly selected for this anatomic study. Among these specimens, 2 left shoulders of 2 male cadavers with torn tendons with or without severe degenerative changes were excluded from this study. We used 9 specimens (from 3 male and 2 female cadavers; mean age, 82.0 years) for the morphologic examination (group 1) and 5 specimens (from 1 male and 2 female cadavers; mean age, 71.3 years) for the sectioning study, including frozen section with a diamond saw or histologic staining (group 2).

In the 9 shoulders in group 1, the clavicle and humerus were cut at the proximal portion and the muscles of the shoulder girdle were removed. After the acromion was resected, the fat tissue on the CHL was carefully removed. The specimens were observed with special attention given to the extent of the CHL. In 6 shoulders, the muscular portion of the supraspinatus and subscapularis was gently unraveled in water and removed from the myotendinous units, and the tendons were left attached to the humerus. After the muscle removal, the humerus could be displaced slightly inferiorly so that the extent of the CHL was more clearly observed. The results were recorded with digital photographs (Fig. 1).

In group 2 shoulders, 5 specimens were frozen at  $-80^{\circ}\text{C}$  and serially sectioned (3-mm thickness) with a band saw (WN-25-3; Nakajima Seisakusho, Osaka, Japan) in parallel to the glenoid surface for observations of anteroinferior expansion of the CHL.



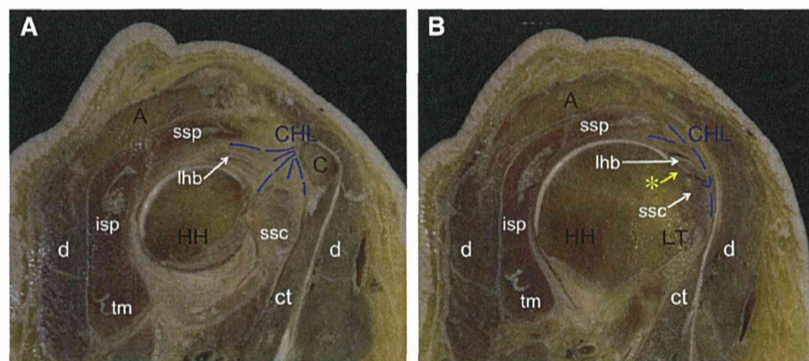


**Figure 2** Macroscopic sagittal sections of shoulder joint. (A) Section at coracoid process (C) near its base. From the rotator interval, the CHL extended below the supraspinatus muscle (ssp) and ran from the anterior to posterior side of the subscapularis muscle. (B) Section at lesser tuberosity (LT). The subscapularis tendon was located on the lesser tubercle and extended as a tendinous slip to the top of the intertubercular groove (yellow asterisk). The long head of the biceps tendon accompanied the gentle slope of the subscapularis tendon. The CHL covered the anterior surface of the subscapularis and made a fold to enter below the long head of the biceps brachii tendon (lhb); it then attached to the tendinous slip of the subscapularis. The CHL enveloped the anterior portion of the supraspinatus (ssp). A, Acromion; ct, conjoined tendon; d, deltoid muscle; HH, humeral head; isp, infraspinatus muscle; ssc, subscapularis muscle/tendon; tm, teres minor muscle.

Afterward, a section series of 3 of 5 shoulders (2 male and 1 female; mean age, 75.0 years) were randomly selected, and histologic analyses were performed. The anterosuperior part of the glenohumeral joint, including the long head of the biceps tendon, and the supraspinatus, subscapularis, coracoid process, and humerus were cut out in every slice between the glenoid and humerus. The portion below the lesser tuberosity was discarded. The constructs of the 3 shoulders were decalcified for 1 week in a solution containing aluminum chloride, hydrochloric acid, and formic acid, as described by Plank and Rychlo.<sup>20</sup> After dehydration, the specimens were embedded in paraffin. The blocks were serially sectioned (5- $\mu$ m thickness) vertically to the most superior intramuscular tendon of the subscapularis. One hundred sections were taken to make sets of each 500- $\mu$ m span. Three sets were stained: one set with Masson trichrome, one set with anti-human type I collagen antibody (F-56; Daiichi Fine Chemical, Toyama, Japan), and one set with anti-human type III collagen antibody (F-58; Daiichi Fine Chemical). Combined antibodies were stained by diaminobenzidine (Histostain-SP kit; Life Technologies, Carlsbad, CA, USA).

In addition, we created group 3, comprising 5 shoulders, to closely measure the dimensions of the CHL on the coracoid process (both sides of 58- and 96-year-old male cadavers and the left side of a 92-year-old female cadaver). The right side of the female specimen was discarded because of a large rotator cuff tear. The coracoid process was harvested at the level of the upper margin of the glenoid and the medial margin of the suprascapular notch with the CHL attached to the process. To observe the attachment area of the CHL, the ligament was meticulously detached with a scalpel from the inferior surface of the horizontal limb and base of the coracoid process. The attachment area of the CHL was marked, and the dimensions were measured with a standard caliper.

## Results

The CHL originated at the horizontal limb and base of the coracoid process. The CHL could be divided into two parts:

one part spread fibers over the rotator interval to the posterior portion of the greater tubercle, and the other part extended fibers to envelop the cranial part of the subscapularis muscle. Moreover, the superficial layer of the latter seamlessly continued to the subscapularis fascia and tightly covered a broad area of the anterior surface of the subscapularis muscle (Fig. 1). By macroscopic analysis of the sagittal sections, the relationship between the subscapularis muscle and CHL mentioned earlier could be confirmed. In addition, at the lateral portion, the subscapularis tendon was located on the lesser tubercle. The tendon of this portion further extended as a tendinous slip, making a gentle slope, and continued to the top of the intertubercular groove. This portion had no cartilage but, rather, had a tendinous floor of the subscapularis slip. The long head of the biceps tendon was situated above this portion. The CHL made a fold to enter the narrow space between the long head of the biceps tendon and subscapularis slope and then attached to the tendinous floor. Consequently, the CHL enveloped the whole subscapularis insertion including the tendinous slip (Fig. 2).

When viewed from the inferior side, the CHL attachment was composed of a narrow anteromedial part and a broad lateral part. The anteromedial part of the CHL attached to the anterior edge of the inferior surface of the coracoid process. The lateral part attached to the lateral one-third area of the inferior surface of the horizontal limb of the process (Fig. 3). The mean size of the coracoid process and the dimensions of the CHL are listed in Table I.

During the histologic investigation, the CHL was identified at the rotator interval and it was found to encircle the subscapularis muscle. The ligament consisted of irregular and sparse fibers and did not show the typical ligamentous structure of parallel bundles as described in a previous article.<sup>10</sup> The portion around the long head of the biceps

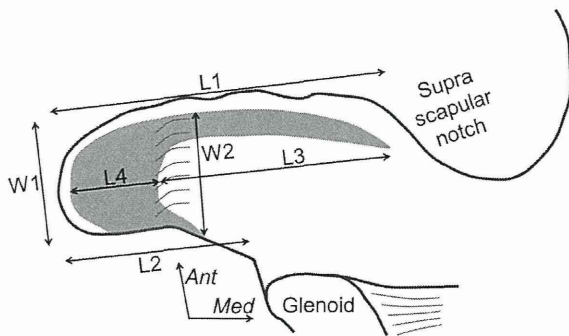


**Figure 3** Schematic illustration of dimensions of CHL on inferior surface of coracoid process. The inferior surface of the right coracoid process is shown. The typical attachment of the CHL is shown as the gray area. The locations for the measurements are listed in Table I. Ant, Anterior; Med, medial.

tendon near the humerus contained relatively dense fibers, but the border between the CHL and the superior glenohumeral ligament was not distinct even by histologic analysis. Immunohistologically, the CHL stained more densely for type III collagen than the subscapularis or the long head of the biceps tendon (Fig. 4).

## Discussion

Several previous reports have indicated that the CHL attaches to the subscapularis muscle. Harryman et al<sup>13</sup> described that the CHL divides into two major bands, one of which inserts into the tendinous anterior edge of the supraspinatus and the other of which inserts into the superior border of the subscapularis. Yang et al<sup>24</sup> macroscopically showed that the ligament-like portion of the CHL was split and inserted into both the supraspinatus and subscapularis tendons in 3 of 26 fresh-frozen cadavers and that the ligament-like portion inserted into only the subscapularis tendon in 1 specimen. Arai et al<sup>1</sup> reported on the soft tissue composing the CHL, which bridges over the cranial part of the subscapularis muscle. In our study, anteriorly extending fibers of the CHL enveloped the cranial part of the subscapularis muscle, and moreover, the superficial layer of the CHL seamlessly continued to the subscapularis fascia and tightly covered a broad area of the anterior surface of the subscapularis muscle. It is reasonable that the CHL would continue to the subscapularis fascia seamlessly because both of them are composed of loose connective tissue.<sup>10,24</sup> On the basis of the enveloping structure and broad coverage of the subscapularis, the CHL would function as a kind of holder for the subscapularis muscle in the same way in which the ligament works for the supraspinatus muscle.

As shown on a lateral slice of the macroscopic sagittal sections, the subscapularis tendon continued as a tendinous slip from the upper surface of the lesser tubercle to a

**Table I** Dimensions of coracoid process and attachment area of CHL

Location of measurement	Mean $\pm$ SD (mm)
Coracoid process	
Anterior length (L1)	37.5 $\pm$ 6.2
Posterior length (L2)	23.8 $\pm$ 1.8
Anteroposterior width (W1)	16.5 $\pm$ 2.5
Attachment of CHL	
Length of anteromedial part (L3)	18.6 $\pm$ 6.1
Length of lateral part (L4)	10.3 $\pm$ 1.9
Anteroposterior width of lateral part (W2)	13.5 $\pm$ 1.4

The locations of the specific measurements are shown in Fig. 3.

cartilage-lacking portion of the superior intertubercular groove, which corresponded to the fovea capitis of the humerus, and formed a tendinous floor. The CHL was noted to enter below the long head of the biceps tendon and to attach to the tendinous floor. Regarding the tendinous slip of the subscapularis, our finding is supported by previous anatomic studies, and for the tissue that attaches to the tendinous slip, these previous articles claimed that it was the superior glenohumeral ligament.<sup>1,2</sup> In contrast, we did not find the connection of the superior glenohumeral ligament; rather, we found a direct connection of the CHL to the tendinous slip, although according to our histologic results, the portion of relatively dense fibers around the long head of the biceps tendon seemed to correspond to the superior glenohumeral ligament. This difference might appear paradoxical.

To resolve the inconsistency of the results between previous studies and our study, we must first confirm some premises. Classically, the superior glenohumeral ligament was thought to have 3 basic types of origin: (1) the middle glenohumeral ligament, long head of the biceps tendon, and superior labrum; (2) the long head of the biceps tendon and superior labrum; and (3) the long head of the biceps tendon only.<sup>8</sup> At the lateral rotator interval, the superior glenohumeral ligament was classically thought to be in close contact with the CHL because some articles insisted that they were tightly united.<sup>17,22</sup> Recently, both the superior glenohumeral ligament and the CHL were thought to be components of the same loose connective tissue rather than the unity of 2 independent structures.<sup>1</sup> In addition, Pouliart et al<sup>21</sup> proposed the concept of these ligaments as 1 ligamentous structure with variable parts, and furthermore, our histologic study did not find any clear border for the superior glenohumeral ligament in the CHL. These newer studies and our histologic results suggest that the superior glenohumeral ligament may simply be a limited portion of the CHL, which attaches to the tendinous slip of the subscapularis.